

Structural studies of polysiloxanes: crystal structure and fold conformation of poly(tetramethyl-*p*-silphenylene siloxane)

K. H. Gardner*, J. H. Magill† and E. D. T. Atkins

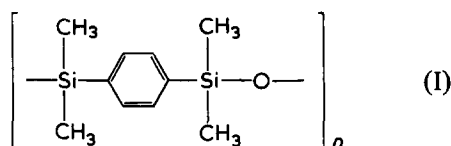
H. H. Wills Physics Laboratory, University of Bristol, Royal Fort, Tyndall Avenue, Bristol BS8 1TL, UK

(Received 18 August 1977; revised 6 October 1977)

The crystal structure of poly(tetramethyl-*p*-silphenylene siloxane) has been determined using X-ray diffraction data from drawn fibres. The unit cell is tetragonal with dimensions $a = b = 0.902$ nm and c (fibre axis) = 1.543 nm. The space group is $P4_32_12$ and the unit cell contains four monomer units. Each chain adopts a 2_1 helical conformation so that two chains run through the unit cell. The crystallographic asymmetric portion of the molecule is one half of a monomer unit with the oxygen atom and the centre of mass of the phenyl group at special positions. The two halves of a monomer are symmetry related by a diad axis perpendicular to the fibre axis. In addition, this polymer [poly(TMPS)] can crystallize in the form of chain-folded lamellae, and detailed models for the fold structure have been examined using computer model building techniques. A unique conformational model was found for adjacent re-entry fold models and a stereochemically acceptable fold can be obtained using a single residue. The only acceptable models encompassing two or three residues in the fold turn out to be only small perturbations of the single residue adjacent re-entry fold.

INTRODUCTION

Although structural information on inorganic silicon compounds is abundant in the literature¹, detailed X-ray diffraction studies of organosilicon polymers is very limited. A current comprehensive review² of crystallographic data for polymeric materials lists only two citations relating to polysiloxanes, namely, poly(dimethyl siloxane)^{3,4} and poly(dipropyl siloxane)⁵. This paucity of data in no way reflects the industrial interest, technological importance or future potential of silicon-containing polymers. On the academic side the chemistry and material science aspects of polysiloxanes have received much attention over the years^{6,7}. In particular poly(tetramethyl-*p*-silphenylene siloxane) (I), hereafter denoted poly(TMPS), has incited interest because of its desirable physical properties.



As a block copolymer with dimethyl siloxane it was one of the earliest polysiloxanes of its kind to be synthesized.

Fractions of poly(TMPS) homopolymer have been studied in some detail over the last decade^{8,9}. Crystallization kinetics⁸, spherulitic and single crystal morphology¹⁰, glass tran-

sition temperature⁸, melting behaviour¹¹, thermal¹² and chemical stability¹³ feature among some of the investigations carried out to date. The current work was undertaken to provide conformational and structural information on the molecular packing so as to obtain a clearer insight into its properties and physical behaviour. The fact that the melting point and glass transition temperature of poly(TMPS) is considerably higher than in poly(dimethyl siloxane) clearly emphasizes the effect of replacing alternate oxygens in the chain backbone by the rigid phenyl groups. Furthermore, isolated chain-folded lamellar crystals of poly(TMPS) have been found to melt rather than thicken on raising the temperature and this response is likely to be associated with the intricacies of the chain packing in the solid state.

METHODS

Materials and specimen preparation

The preparation of poly(TMPS) has been described previously^{8,14}. The particular specimen used in this work had a viscosity-average molecular weight of 370 000 daltons with a weight- to number-average ratio close to 1.3.

The polymer was melted, cast into a sheet approximately 1 mm thick, and quenched to room temperature where it was allowed to crystallize. Oriented specimens were made by drawing strips of polymer cut from the sheet. The most highly oriented specimen(s) were obtained by holding the stretched strips under constant tension in a spring-loaded stretching device while annealing at 131.5°C in a silicone oil, thermostatically controlled, bath. Material prepared in this way was relatively transparent and did not exhibit discrete small-angle reflections. Its degree of crystallinity, assessed from differential scanning calorimetry, was about 55% and

* Present address: Department of Macromolecular Science, Case Western Reserve University, Cleveland, Ohio 44106, USA.

† Permanent address: Department of Metallurgical and Materials Engineering, School of Engineering, University of Pittsburgh, Pittsburgh, Pennsylvania 15213, USA.

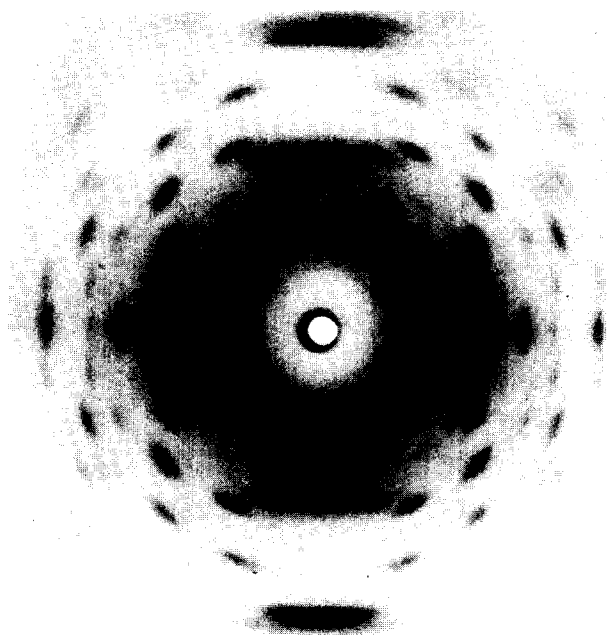


Figure 1 X-ray fibre diffraction photograph from drawn film of poly(TMPS): fibre axis vertical

the density of the oriented strip was found to average 1.064 g/cm^3 when measured in a density gradient column.

X-ray diffraction

Figure 1 shows an X-ray fibre diffraction photograph from stretched poly(TMPS) film recorded on flat film using an Elliott Focussing Toroid camera and Ni-filtered $\text{CuK}\alpha$ radiation. Calcite (characteristic spacing, 0.3035 nm) was used as an internal diffraction standard. From the measured Bragg reflections, the unit cell dimensions were refined by a least squares procedure. Intensities were measured with a Joyce-Loebl microdensitometer. Correction factors for Lorentz polarization, multiplicity and oblique incidence on the film were applied.

Model building

Molecular models for poly(TMPS) were generated using a linked-atom procedure similar to that described by Arnott and Wonacott¹⁵ which has been used in structural investigations of both synthetic¹⁵⁻¹⁷ and biological polymers¹⁸⁻²¹. The positions of the atoms were defined in terms of internal coordinates of the molecule, i.e. bond lengths, bond angles and torsion angles. Bond lengths and, in most cases, bond angles were held constant whilst certain bond angles and torsion angles were treated as refinable parameters. These parameters were varied in order to allow the model to adopt a conformation with the appropriate helix pitch and symmetry while maintaining certain additional symmetry relationships dictated by the space group. The model building was accomplished by varying the refinable parameters so as to minimize the function:

$$\Phi = \sum k_j (\Delta P_j)^2 + \sum \epsilon_n + \sum \lambda_h G_h \quad (1)$$

In this equation the first summation contains a term for each of the varied parameters. The symbol ΔP_j denotes the difference between the standard value for a parameter (determined by a survey of detailed crystal structures of relevant model compounds) and the value of the parameter found

in the molecular model. The weighting constant for the term is represented by k_j .

The second summation in equation (1) is included for the optimization of certain steric features of the model, in a manner similar to that of Guss *et al.*²¹. Through this term close contacts between non-bonded atom pairs could be minimized. While this aspect of the refinement procedure was not used for the refinement of the poly(TMPS) crystal structure, it was used extensively in the determination of plausible fold conformation for poly(TMPS) single crystals (see below).

The third summation contains a series of Lagrangian multipliers λ_h , and constraint expressions, G_h , that must be equated to zero. Through their use, helical symmetry, pitch and chain continuity were imposed on the refining crystal structure models. In addition, certain relationships between molecular parameters, defined by the crystallographic space group symmetry, were imposed on the structure through the appropriate terms in the summation (see Implications of the space group on model building).

For the modelling of fold structures (below) the Lagrangian constraints were used to ensure the proper crystallographic register of poly(TMPS) residues before entering and after leaving the fold. To our knowledge this is the first adaptation of this model building technique to investigate the chain folding of a flexible polymer.

For the structure of poly(TMPS) covalent bond lengths, bond angles and the stereochemistry of rigid groups were based on data obtained from reliable single crystal determinations of relevant low molecular weight compounds²²⁻²⁶. The atomic numbering for poly(TMPS) is illustrated in Figure 2. The phenyl group was fixed as a regular planar hexagon with a C-C (phenyl) distance of 0.140 nm . The silicon atoms were assumed to lie in the same plane as the phenyl ring and to have tetrahedral bonding geometry with a Si-C(phenyl) distance of 0.1858 nm , a Si-C(methyl) dis-

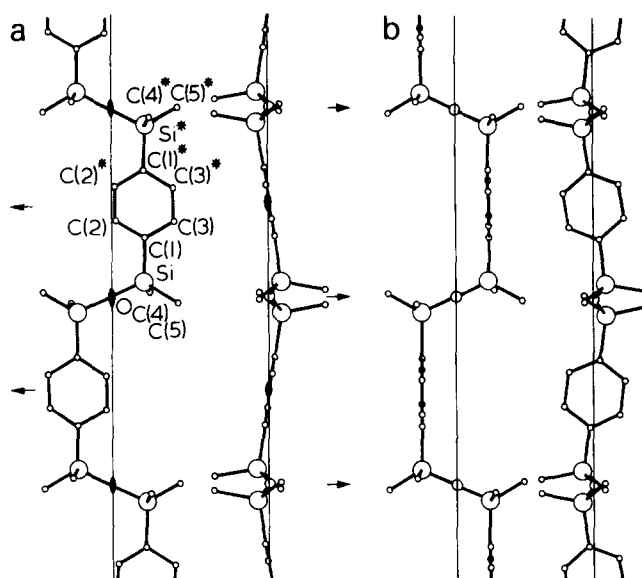


Figure 2 Projections of the two possible conformations for the poly(TMPS) molecule produced by model building. The conformations are the same except for the orientation of the phenyl groups with respect to the rest of the molecule. (a) Model I; (b) Model II. In (a) the two-fold rotation axes perpendicular to the helix axis are indicated (●) when perpendicular to the plane of the page and (→) when parallel to the plane of the page. In some of the projections the oxygen atom is obscured by the (●) symbol

tance of 0.189 nm and a Si–O distance of 0.165 nm. Because of the highly flexible nature of the Si–O–Si bond angle, which will be referred to as $\phi(\text{Si–O–Si})$, this angle was considered to be a variable parameter with a weighting constant k_j equal to 1.0 and a standard value of 144° . Torsion angles about the Si–C(phenyl) and Si–O bonds were also allowed to vary in the model building procedure. Standard values for these torsional angles could not be explicitly defined due to the lack of relevant model compounds. Consequently, k_j , the weighting constant, was set to zero.

In the first section (below) this model building procedure generated models for the poly(TMPS) molecule with $\phi(\text{Si–O–Si})$ as close to 144° as possible whilst *exactly* meeting the constraints placed upon the model. These molecular conformations were used as starting models for the X-ray refinement. In the second section, the model building procedure generated models for the poly(TMPS) fold which were free of over-short, non-bonded contacts and with $\phi(\text{Si–O–Si})$ as close to the value found in the refined crystal structure as possible whilst *exactly* meeting the constraints applied to the model.

X-ray refinement

Applying a procedure similar to that used in the model building, the structural models were refined against the observed X-ray data. Subject to the Lagrangian constraints appropriate to each model, the refinable molecular parameters were adjusted by least squares to produce the 'best fit' between observed and calculated structure factor amplitudes. In order to accomplish this task the function minimized was:

$$\Omega = \sum w_m (\Delta F_m)^2 + \sum \lambda_h G_h \quad (2)$$

where in the first summation ΔF_m is the difference between the observed and calculated structure factor amplitude for the m th reflection and w_m is the weight to be applied to the observation. For this refinement a unit weighting scheme was employed. In addition to the molecular parameters, the average isotropic temperature factor and crystallographic scale factors were also refined. The second term in equation (2) contains a summation comprising of Lagrangian constraints (G_h) and multipliers (λ_h) similar to those used in the model building procedure.

The resulting models were assessed in the conventional manner using the residual factors (R and R'') given by

$$R = \sum |\Delta F_m| / \sum F_m(\text{obs}), \quad (3)$$

and

$$R'' = \{ \sum w_m (\Delta F_m)^2 / \sum w_m [F_m(\text{obs})]^2 \}^{1/2} \quad (4)$$

CRYSTAL STRUCTURE OF POLY(TMPS)

Unit cell and space group

The Bragg reflections were indexed by a tetragonal unit cell with dimensions $a = b = 0.902$ nm and $c(\text{fibre axis}) = 1.543$ nm. The first meridional (001) reflection lies on the fourth layer line. Equatorial ($h00$) reflections are observed only when $h = 2n$. These selection rules suggest that the space group is either $P4_12_12$ or $P4_32_12$. In both space groups there are eight equivalent general positions in the unit cell and four equivalent special positions.

The calculated density based on four monomer units in

the unit cell, is 1.103 g/cm³ which is in agreement with the observed density of the drawn fibre (1.064 g/cm³), considering that highly drawn synthetic fibres usually possess a relatively high void content.

Implications of the space group on model building

While space group symmetry requires the presence of eight equivalent atomic positions, the density measurements show that there are four monomers in the cell thus indicating that the crystallographic asymmetric portion of the molecule is one half of the monomer unit. Since the monomer contains only one oxygen and one phenyl ring, the centre of mass of the phenyl ring and the oxygen must lie on crystallographic special positions which are:

$$(x, x, 0; x, x, 1/2; 1/2 - x, 1/2 + x, 1/4; 1/2 + x, 1/2 - x, 3/4)$$

or

$$(x, x, 0; x, x, 1/2; 1/2 - x, 1/2 + x, 3/4; 1/2 + x, 1/2 - x, 1/4)$$

for space groups $P4_12_12$ and $P4_32_12$, respectively. These special positions correspond to the points along diad axes that are mutually perpendicular to each other and to the fibre axis which they intercept every $c/4$. The diad axes are oriented along the diagonals of the ab projection of the unit cell.

In a unit cell with $P4_12_12$ or $P4_32_12$ symmetry the cell contents can be distributed in two ways that are consistent with the formation of continuous helices. Either the four residues could form a four-fold helix passing through the point $(1/2, 0, 0)$. In this case the choice of space group would depend on whether the helices were left- or right-handed. Alternatively, the unit cell could contain 2 two-fold helices passing through the corners and centre of the unit cell with the chain at the centre of the cell having a relative translation of $+c/4$ ($P4_12_12$) or $-c/4$ ($P4_32_12$) with respect to the chain at the origin. It is not possible to construct a four-fold helix, meeting the special symmetry requirements placed on the positions of the oxygens and phenyl groups. Thus the structure was concluded to consist of two-fold helices. Since the difference between the two space groups involves only the packing of chains in the unit cell, the choice of space group will be deferred to a later section.

In addition to the restrictions imposed on the molecule by two-fold helical symmetry, the diad axis passing through the oxygen requires that $\theta[\text{C}(1), \text{Si}, \text{O}, \text{Si}^*]$ be equal to $\theta[\text{Si}, \text{O}, \text{Si}^*, \text{C}(1)^*]$. Even more stringent requirements are imposed on the orientation of the phenyl rings. Not only must the centre of mass of the phenyl group lie on a diad axis, but the plane of the ring must lie either perpendicular to the diad axis or contain it. These orientations place exact constraints on the allowable values for the torsion angles about the Si–C(phenyl) bonds. If the diad axis lies in the plane of the phenyl ring then $\theta[\text{C}(2), \text{C}(1), \text{Si}, \text{O}]$ must be equivalent to $\theta[\text{C}(2)^*, \text{C}(1)^*, \text{Si}^*, \text{O}]$. Alternatively, if the ring is perpendicular to the diad then $\theta[\text{C}(2), \text{C}(1), \text{Si}, \text{O}]$ will equal $\theta[\text{C}(2)^*, \text{C}(1)^*, \text{Si}^*, \text{O}] + 180^\circ$.

Molecular models

Two-fold helical models for poly(TMPS) were constructed based on the experimentally determined pitch and the torsional angle constraints detailed in the preceding section. The molecular variables were: (i) the Si–O–Si bond angle,

Table 1 Non-bonded intramolecular distances shorter than 0.38 nm

Model 1		Model 2	
O ... C(2)	0.318 nm	O ... C(2)	0.348 nm
C(3) ... C(4)	0.378 nm	C(2) ... C(5)	0.349 nm
C(3) ... C(5)	0.337 nm	C(3) ... C(4)	0.324 nm
C(4) ... C(4)*	0.334 nm ^a	C(4) ... C(4)*	0.334 nm ^a

^a The contact is between C(methyl) atoms which are related by the diad axis through the oxygen atom

$\phi(\text{Si}, \text{O}, \text{Si}^*)$; (ii) the torsion angles about the Si–O bonds; (iii) the torsion angles about the Si–C(1) bonds.

For the isolated chain, it was found that only two conformations were stereochemically feasible. These conformations, designated as models I and II, are illustrated in Figure 2. The non-bonded intrachain contact distances for the models are listed in Table 1.

Model I incorporates the following features: (a) the oxygen atoms lie on the helix axis; (b) the oxygen bond angle [$\phi(\text{Si}, \text{O}, \text{Si}^*)$] is 143.6° ; (c) the phenyl group is displaced from the helix axis and (d) the plane of the phenyl ring contains the diad axis that passes through the centre of mass of the group. Consequently, the plane of the phenyl group lies perpendicular to the two-fold axis passing through the oxygen (see Figure 2a).

Model II is shown in Figure 2b. In this model the plane of the phenyl group is perpendicular to the diad axis through the ring, otherwise the chain conformation is the same as Model I.

For the sake of completeness an alternative molecular model which was rejected on stereochemical grounds will be briefly described. This is the special case when $\theta[\text{C}(2), \text{C}(1), \text{Si}, \text{O}] = \theta[\text{C}(2)^*, \text{C}(1)^*, \text{Si}, \text{O}] = 180^\circ$. In such a model the $\text{C}(1)^*-\text{Si}^*-\text{O}-\text{Si}-\text{C}(1)^*$ moiety is planar and the centres of the phenyl groups lie on the helix axis. However, in order to match the observed fibre repeat in poly(TMPS), it is necessary to compress the Si–O–Si bond angle to 122.3° , an unacceptably small value for this bond angle. Consequently models containing this feature were rejected.

Structure refinement

Chain models were placed in the unit cell at the packing positions dictated by the possible space groups $\text{P}4_12_12$ and $\text{P}4_32_12$. Least squares X-ray refinements were made on the four packing models, i.e. model I($\text{P}4_12_12$), model I($\text{P}4_32_12$), model II($\text{P}4_12_12$) and model II($\text{P}4_32_12$). (The space group in which the model was packed is in parenthesis.) In undertaking these refinements the same molecular parameters were varied as in the model building procedure. However, the Si–Si bond angle was allowed to assume any value that would improve the agreement between the observed and calculated structure amplitudes. The overall isotropic temperature factor was also allowed to change during the refinements. The packing parameters of rotation about, and translation along, the helix axes were invariant and defined by space group symmetry.

Model I($\text{P}4_32_12$) was found to give the best agreement with the observed X-ray data ($R = 0.210$ and $R'' = 0.191$)[‡].

[‡] The structure that gave the next best agreement with the observed X-ray data was model II($\text{P}4_32_12$) with $R = 0.342$ and $R'' = 0.332$. In addition to the higher R values this model has a C(methyl)–C(phenyl) interchain contact of 0.292 nm.

The resulting structure has only one interchain contact of less than 0.38 nm: a C(methyl)–C(phenyl) contact of 0.352 nm. Even though the molecular parameters were allowed to vary, the conformation of the chain did not alter significantly during the X-ray refinement from the structure for Model I shown in Figure 2a. The final coordinates of the structure are tabulated in Table 2. A comparison of the observed and calculated structure factor amplitudes is listed in Table 3.

The molecular arrangement in crystalline poly(TMPS), observed perpendicular to the ab and ac planes, is shown in Figure 3. Considering the chain at the corner of the unit cell, the oxygen atoms lie on the helix axis at the positions (0, 0, 0) and (0, 0, 1/2). The bond angle at the oxygen atom [$\phi(\text{Si}, \text{O}, \text{Si}^*)$] is 143.6° and is bisected by a diad axis that lies perpendicular to the chain axis. The centres of mass of the phenyl groups lie in the (110) plane on diad axes that intersect the chain axis at $z = 1/4$ and $z = 3/4$. The final values for the refined torsional angles are:

$$\theta[\text{C}(1), \text{Si}, \text{O}, \text{Si}^*] \{ = \theta[\text{Si}, \text{O}, \text{Si}^*, \text{C}(1)^*] \} = 107.1^\circ$$

and

$$\theta[\text{C}(2), \text{C}(1), \text{Si}, \text{O}] \{ = \theta[\text{C}(2)^*, \text{C}(1)^*, \text{Si}^*, \text{O}] \} = -23.1^\circ$$

The conformation of the isolated monomer is very similar to that of the monomer found in poly(TMPS). The value for the torsional angle about the Si–C bond is -11.5° (as compared to -23.1° in the polymer). In the structure of the monomer the oxygen is found as a hydroxyl group and the molecular conformation is stabilized by intermolecular hydrogen bonds²⁴.

Table 2 Positional parameters (fractional coordinates) for atoms in an asymmetric unit and consisting of one half of a poly(TMPS) monomer unit^a

Atom	X	Y	Z
O ^b	0.0000	0.0000	0.0000
Si	-0.1526	0.0717	0.0415
C(1)	-0.1296	0.0947	0.1604
C(2)	-0.0258	0.0084	0.2052
C(3)	-0.2160	0.1984	0.2052
C(4)	0.2585	-0.1892	0.0098
C(5)	-0.0560	-0.3142	-0.0193

^a The space group is $\text{P}4_32_12$. The remainder of the scattering material in the unit cell can be generated by the following symmetry elements:

$$y, x, z; \bar{x}, \bar{y}, \frac{1}{2} + z; \bar{y}, \bar{x}, \frac{1}{2} - z; \frac{1}{2} - y, \frac{1}{2} + x, \frac{3}{4} + z;$$

$$\frac{1}{2} - x, \frac{1}{2} + y, \frac{3}{4} - z; \frac{1}{2} + y, \frac{1}{2} - x, \frac{1}{4} + z; \frac{1}{2} + x, \frac{1}{2} - y, \frac{1}{4} - z$$

With the first symmetry element the complementary half of the monomer unit can be produced. The second and third elements generate the second monomer of the chain at the origin, and the last four elements generate the second chain in the centre of the unit cell.

^b This atom is at a special position and found at

$$0, 0, \frac{1}{2}; \frac{1}{2}, \frac{1}{2}, -\frac{1}{4}; \frac{1}{2}, \frac{1}{2}, \frac{1}{4}$$

Table 3 Observed and calculated^a structure factor amplitudes for poly(TMPS)

<i>h</i>	<i>k</i>	<i>l</i>	<i>F</i> (obs)	<i>F</i> (calc)	<i>h</i>	<i>k</i>	<i>l</i>	<i>F</i> (obs)	<i>F</i> (calc)
1	0	0	sa ^b	0	3	1	2	260	150
1	1	0	1000	998	3	2	2	50	142
2	0	0	150	130					
2	1	0	940	821	0	0	3	sa	0
2	2	0	330	355	1	0	3	130	196
3	0	0	sa	0	1	1	3	60	102
3	1	0	180	113	2	0	3	40	52
3	2	0	380	321	2	1	3	310	297
					2	2	3	80	118
0	0	1	sa	0	3	0	3	140	116
1	0	1	180	202	3	1	3	180	180
1	1	1	440	583					
2	0	1	440	437	0	0	4	vs	891
2	1	1	360	413	1	0	4	100	119
2	2	1	— ^c	59	1	1	4	180	209
3	0	1	—	117	2	0	4	—	16
3	1	1	170	127	2	1	4	230	182
3	2	1	250	255	2	2	4	60	152
					3	0	4	—	92
0	0	2	sa	0	3	1	4	70	157
1	0	2	470	377					
1	1	2	170	103	0	0	5	sa	0
2	0	2	160	224	1	0	5	—	29
2	1	2	230	149	1	1	5	170	199
2	2	2	160	208	2	0	5	170	111
3	0	2	—	37	2	1	5	50	113

^a Atomic scattering factors were calculated using an analytical approximation, taken from International Tables²⁷; ^b Systematically absent reflections; ^c The symbol (—) indicates reflections that were not observed above the background scatter on the X-ray film. When these reflections were included in the X-ray refinement as observed reflections with unit weights and intensity of 0.0, the values of *R* and *R*' were 0.253 and 0.211, respectively but the model remained unchanged

DETAILED MODEL FOR THE FOLD CONFORMATION OF POLY(TMPS)

Poly(TMPS) can be crystallized in chain-folded lamellae from solution and melt¹⁰ in which the chains fold in the (110) plane similar to the lamellar crystals of carbon-based synthetic polymers^{28,29}. An electron micrograph and corresponding diffraction pattern, illustrative of the tetragonal symmetry of these crystals are shown in *Figure 4*. A projection of the (110) 'fold plane' of poly(TMPS), as established by this structure determination, is shown in *Figure 5*. There is an accumulation of evidence that the folds connecting these 'stems' are tight (i.e. containing as low as one or two monomer units) and the surface is relatively regular^{13,30}. To construct a detailed model for the fold of the poly(TMPS) molecule as found in chain-folded lamellar crystals there are certain criteria which an acceptable fold model must meet.

(i) The molecule must occupy a crystal lattice site in the structure in the (110) plane before entering and after leaving the fold. (Because of the apparent tight folding only adjacent re-entry models are considered.)

(ii) Over-short non-bonded intramolecular contacts should be avoided and bond angle distortion should be kept to a minimum.

(iii) There should be no over-short contacts between atoms in adjacent folds on a regular fold surface.

(iv) The number of residues involved in the fold should be small.

These criteria for an acceptable model limit the number of possible fold types. Since there is a quarter stagger along the *c*-axis between a particular chain and its near neighbours, to the left and right in the (110) fold plane (see *Figure 5*) it is possible for the fold to terminate at a residue in an adjacent

straight stem that is staggered up or staggered down relative to fold-initiating residue. (Due to the two-fold helical nature of the model, there are no other new fold possibilities to be considered if another residue in the straight stem was chosen as the starting point for a fold).

Models were constructed for each of these fold types, incorporating one, two and three residues within the fold. The extremes of the fold were defined by having the phenyl groups of the fold-initiating and fold-terminating residues in the crystal lattice (straight-stems) and allowing free rotation about the Si—C(phenyl) bonds to these residues.

Of the possible single residue folds only one satisfied the imposed constraints and such a structure is illustrated in *Figure 6*. The coordinates of the atoms in the fold are listed in *Table 4*. The model is free of non-bonded steric interferences (i.e. no non-bonded contacts of less than 0.32 nm). In addition the model was constructed without distortion of the Si—O—Si bond angles from 143.6°, the value for the bond angle found in our refined crystal structure.

The manner in which a chain would be incorporated into a folded-chain lamellar crystal is shown schematically in *Figure 7*. This illustrates part of a (110) plane of a poly(TMPS) chain-folded lamella. The chain shown in *Figure 7* constitutes four straight stems in the arrangement determined by the crystal structure analysis and three folds in the conformation determined in this study. *Figure 8* shows the appearance of a regular fold surface of a lamellar single crystal which incorporates our proposed fold structure.

The investigation of folds incorporating two and three residues produced models which deviated minimally from the single-residue fold. Only small perturbations of the molecular parameters of the fold-initiating and fold-terminating residues defined for the single-residue fold were found.

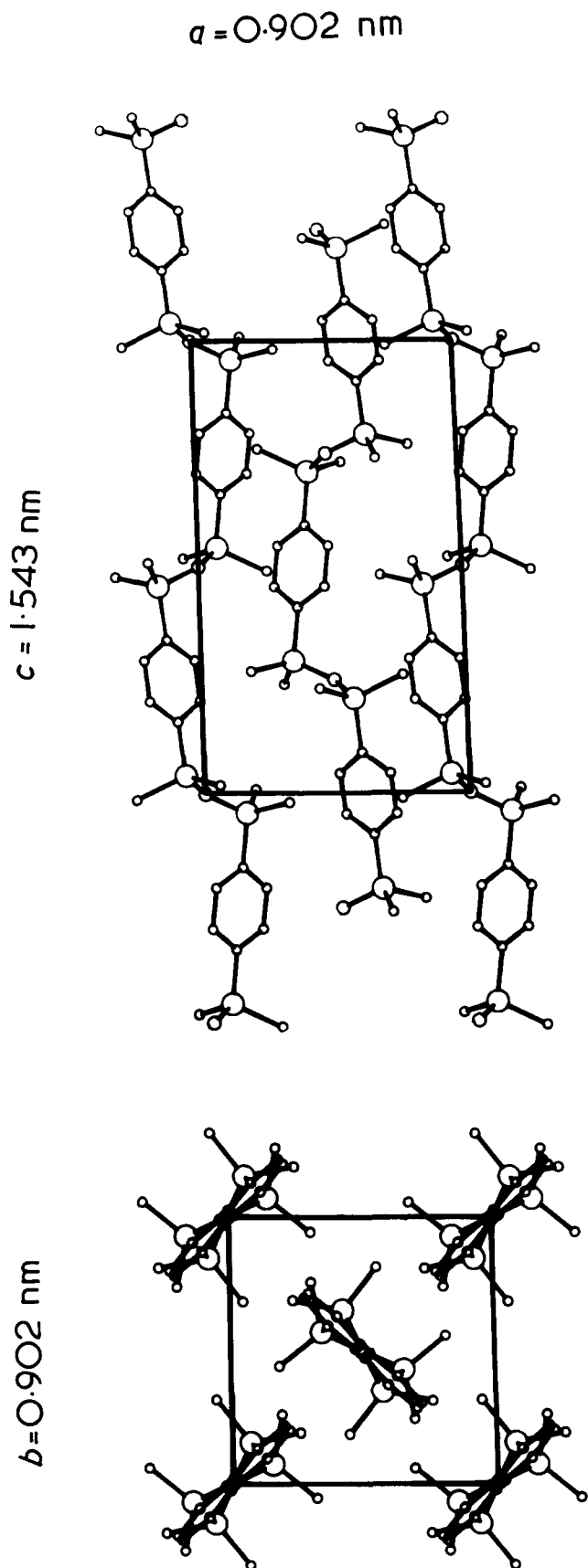


Figure 3 Crystal structure of poly(TMPS). (a) The ac projection is shown (perpendicular to fibre axis) and (b) the ab projection, looking down fibre axis, is shown

Poly(TMPS), like most other crystallizable polymers, crystallizes from several solvents giving well developed solution grown crystals under suitable conditions. As in many carbon-based polymers, these crystals have growth faces consisting of $\{110\}$ crystallographic planes in which the polymer chain folds to a length dictated by the undercooling below the thermodynamic solution temperature of an ideal crystal. Although poly(TMPS) tends to be a 'stiffer' molecule than poly(dimethyl siloxane) the inherent flexibility of the Si—O—Si bond in both monomer units, with its attendantly large bond angle, allows the molecule to fold with comparative ease. Based upon the work of chain folding, deduced from crystal growth rate measurements, it follows that poly(TMPS) has a small q parameter (work of chain folding), lower than most other polymers. This is consistent with the calculated projection of the (110) fold plane in poly(TMPS) (based on bond angles and bond distances) clearly illustrates this point (see Figure 7). However, translation of such a molecule through the lattice of a single crystal must be less facile in this siloxane than in polyethylene even when the differences in chain cross-section are considered. Based upon the current X-ray structure study, it appears that the intermeshing of non-bonded methyl groups plus the added size and 'inherent stiffness' imparted by the phenyl rings in the crystalline state, must oppose solid state self-diffusion below

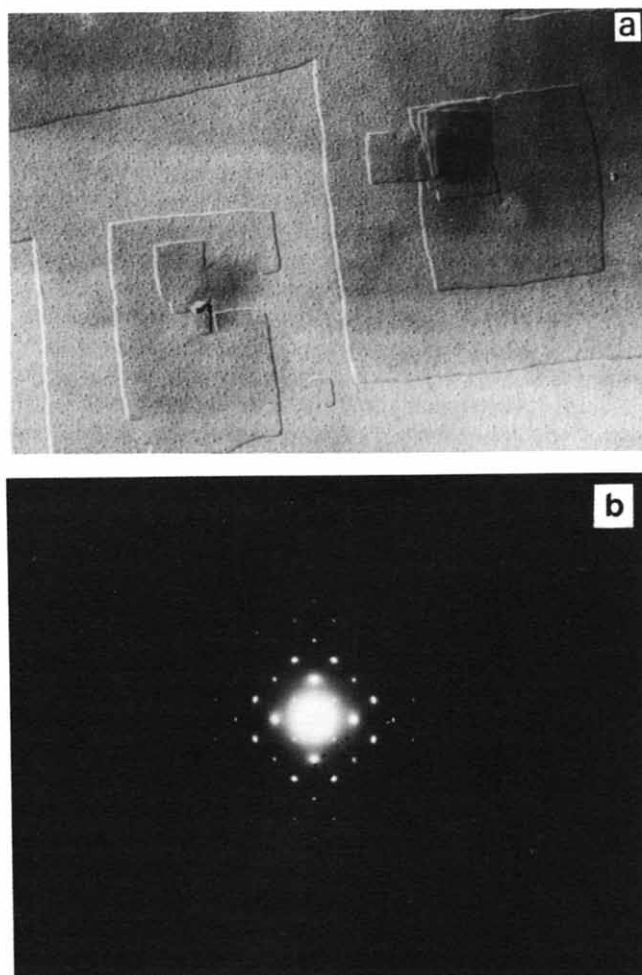


Figure 4 (a) Electron micrograph of shadowed poly(TMPS) single crystals prepared from benzene—methanol solution at 25°C . (b) Corresponding electron diffraction pattern from the same specimen at 100 kV

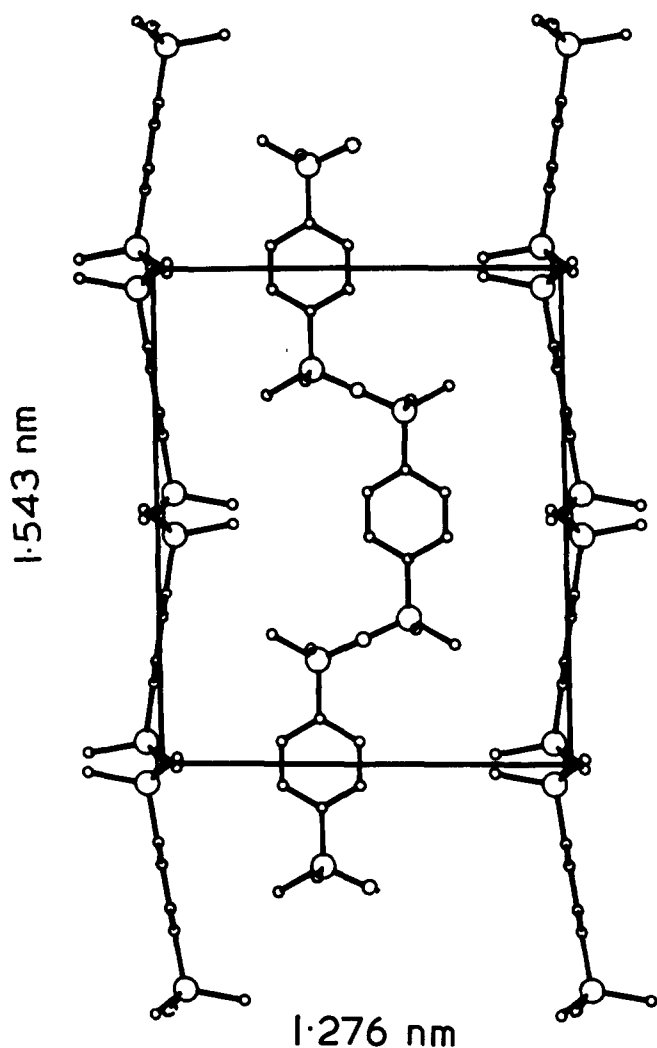


Figure 5 Projection of the molecules in the (110) plane. This plane corresponds to the 'fold plane' in poly(TMPS) single crystals

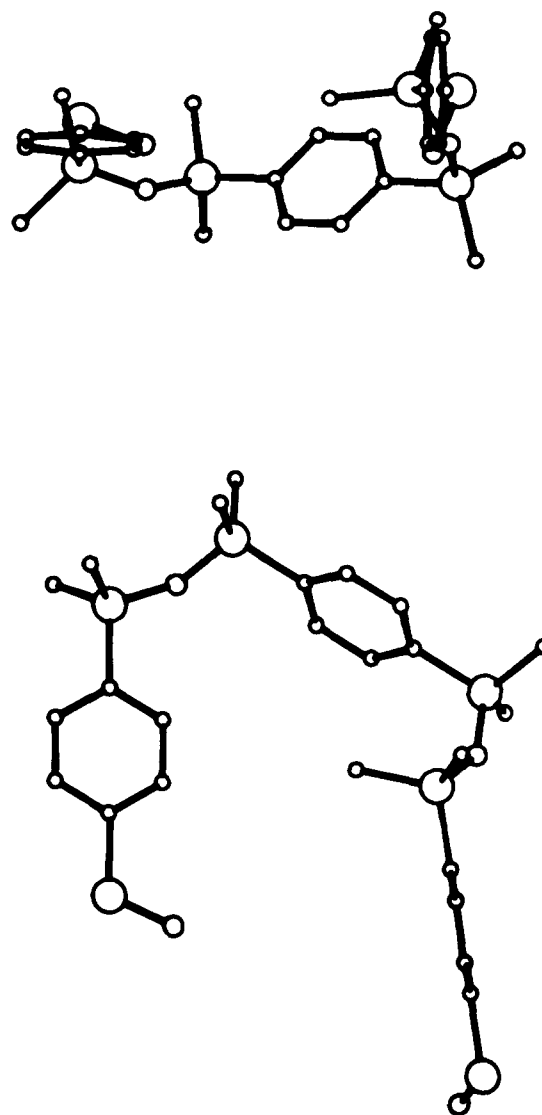


Figure 6 Conformation of poly(TMPS) fold containing single residue

Table 4 Coordinates of the atoms in the single-residue fold of poly(TMPS). Residue one (fold-initiating residue). Residue two (fold residue). Residue three (fold-terminating residue)

Atom	x(X 10 ⁴ nm)	y(X 10 ⁴ nm)	z(X 10 ⁴ nm)	Atom	x(X 10 ⁴ nm)	y(X 10 ⁴ nm)	z(X 10 ⁴ nm)
Residue one:							
O	0	0	0	Si*	4076	3099	12419
Si	-1374	645	639	C(1)*	2937	1972	11480
C(1)	-1166	853	2474	C(2)*	3451	1090	10546
C(2)	-241	83	3157	C(3)*	1573	2015	11713
C(3)	-1936	1778	3159	C(4)*	4043	2653	14220
C(4)	2332	-1707	151	C(5)*	3521	4857	12209
C(5)	-505	-2834	-298				
Si*	-646	1373	7055	Residue three:			
C(1)*	-854	1650	5221	O	5183	3745	11388
C(2)*	-84	24	4538	Si	5883	5156	10913
C(3)*	-1779	1935	4538	C(1)	5675	5364	9078
C(4)*	-2174	2148	7768	C(2)	4750	4594	8395
C(5)*	814	2466	7393	C(3)	6445	6289	8395
				C(4)	7691	5122	11329
Residue two:				C(5)	5074	6575	11791
O	-401	-98	7751	Si*	5155	5884	4497
Si	91	-842	9132	C(1)*	5363	5676	6331
C(1)	1230	285	10072	C(2)*	4593	4751	7015
C(2)	2594	242	9838	C(3)*	6288	6446	7015
C(3)	716	1167	11006	C(4)*	6807	6210	3719
C(4)	987	-2410	8705	C(5)*	4021	7313	4161
C(5)	-1386	-1241	10181	O	4510	4510	3858

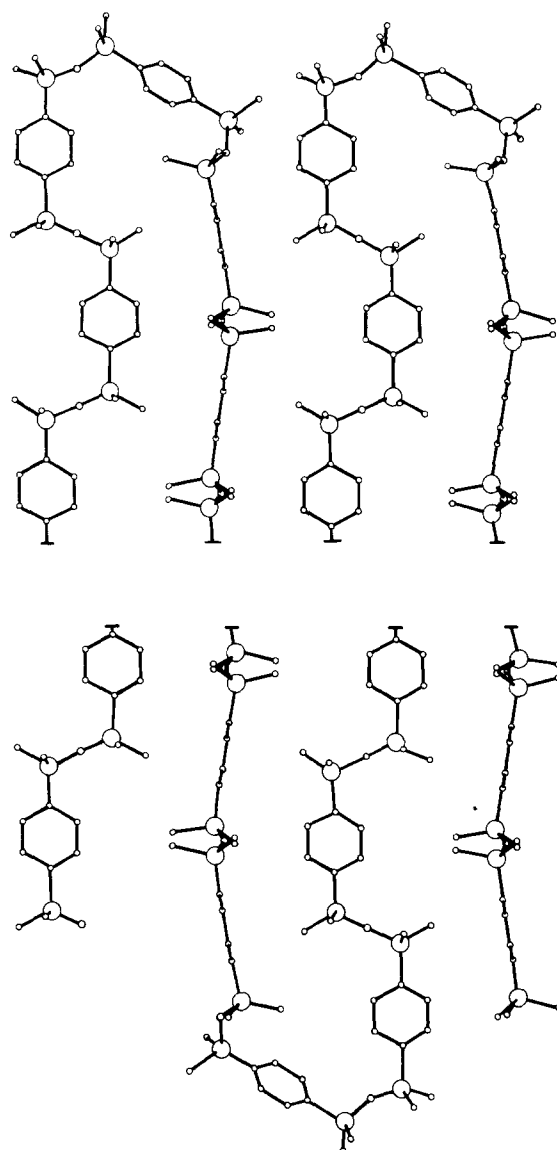


Figure 7 Projection of the (110) plane of a hypothetical chain-folded single crystal showing the way in which the folds combine with the known crystal structure to make up the complete lamellar crystal

the material melting point. Early observations made during the annealing of isolated solution grown crystals are consistent with that rationale, since these crystals only appear to thicken after melting. Overall then, it is clear that not only is a knowledge of poly(TMPS) structure important in its own right but it has far reaching morphological implications.

CONCLUSIONS

Poly(TMPS), like most carbon-based polymers, form chain-folded crystals under suitable conditions¹⁰. As in carbon-based polymers, these crystals have growth faces consisting of {110} crystallographic planes in which the polymer molecule folds. A projection of the (110) 'fold plane' of poly(TMPS) is shown in Figure 7. One of the striking features of the molecular conformation can be seen in this projection. The methyl groups of adjacent chains intermesh to a very high degree. While crystals of carbon-based polymers are observed to thicken on annealing at temperatures near the melting point of the polymers³¹. Poly(TMPS) melts before any thickening occurs. The intermeshing of the

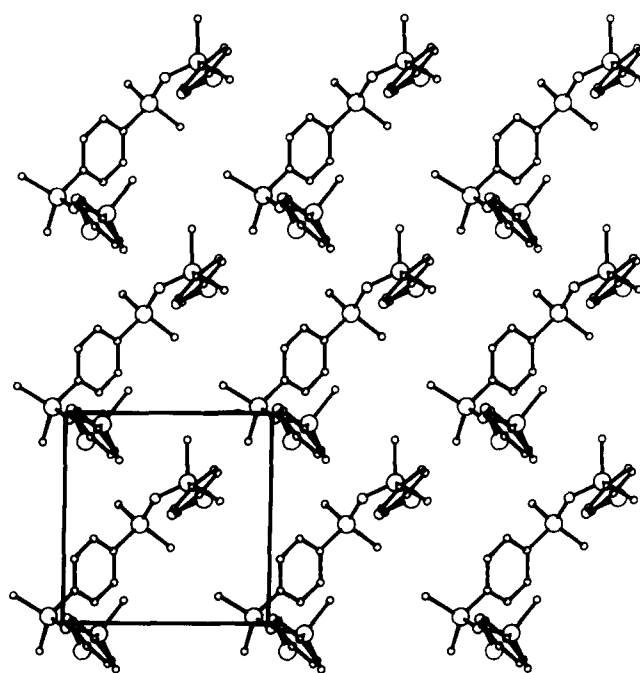


Figure 8 Topological map of a regular chain-folded poly(TMPS) crystal. The square box indicates the position of the unit cell for the crystalline stems relative to the fold surface

methyl groups, when combined with the overall stiffness given to the chain by the systematic inclusion of phenyl groups in the backbone would make the self-diffusion of the molecule extremely difficult and would preclude the thickening phenomenon.

A structure for the chain fold in lamellar single crystals of poly(TMPS) based on adjacent re-entry, has been described. This model building was possible since the detailed crystal structure of the straight stem segments was elucidated. Thus the complete stereochemistry of a chain-folded lamella has been established using model building procedures coupled with X-ray diffraction techniques. It would seem appropriate in the light of this investigation that the application of a similar methodology to other polymeric systems could provide a better understanding of the nature of the fold surface and structure of lamellar single crystals.

ACKNOWLEDGEMENT

We thank the Science Research Council for support.

REFERENCES

- 1 Dunnavant, W. R. *Inorg. Macromol. Rev.* 1971, p 165
- 2 Miller, R. L., in 'Polymer Handbook' 2nd Edn (Eds Brandrup, J. and Immergut, E. H.), 1974, Section 3-1
- 3 Damaschum, G., *Kolloid Z.* 1972, **180**, 65
- 4 Andrianov, K. A., Slonimskii, G. L., Zhdanov, A. A., Levin, V. Yu., Godovskii, Yu. K. and Maskalenko, V. A. *J. Polym. Sci. (A-1)* 1972, **10**, 1
- 5 Lee, C. L., Johannson, O. K., Flaningam, O. L. and Hahn, P. *Polym. Prepr.* 1969, **10**, 1319; Petersen, D. R., Carter, D. R. and Lee, C. L. *J. Macromol. Sci. (B)* 1969, **3**, 519
- 6 Andrianov, K. A. and Petrashko, A. I., *Russ. Chem. Revs. (English Trans.)* 1969, **30**, 211
- 7 Balykova, T. N., and Rode, V. V. *Russ. Chem. Revs. (English Trans.)* 1969, **38**, 306
- 8 Magill, J. H. *J. Appl. Phys.* 1964, **35**, 3249; *J. Polym. Sci. (A-2)* 1967, **5**, 89
- 9 Kojima, M., Magill, J. H. and Merker, R. L. *J. Polym. Sci. (A-2)* 1974, **12**, 317
- 10 Haller, M. and Magill, J. H. *J. Appl. Phys.* 1969, **40**, 4261

Structural studies of polysiloxanes: K. H. Gardner et al.

- 11 Magill, J. H. unpublished results
- 12 Funt, J. M., Parekh, R. D., Magill, J. H. and Shah, Y. T. *J. Polym. Sci. (A-1)* 1975, **13**, 2181
- 13 Okui, N. and Magill, J. H. *Polymer* 1976, **17**, 1086
- 14 Merker, R. L. and Scott, M. J. *J. Polym. Sci. (A)* 1964, **2**, 15
- 15 Arnott, A. and Wonacott, A. J. *Polymer* 1966, **7**, 157
- 16 Takahashi, Y., Sato, T., Tadokoro, H. and Tanaka, Y. *J. Polym. Sci. (A-2)* 1973, **11**, 233
- 17 Claffey, W., Gardner, K. H., Blackwell, J., Lando, J. B. and Geil, P. H. *Phil. Mag.* 1974, **30**, 1223
- 18 Arnott, S., Dover, S. D. and Elliott, A. *J. Mol. Biol.* 1967, **30**, 201
- 19 Arnott, S. in 'Progress in Biophysics and Molecular Biology', Pergamon, Oxford, 1970, **21**, 267-319
- 20 Gardner, K. H. and Blackwell, J. *Biopolymers* 1974, **13**, 1975
- 21 Guss, M. J., Hukins, D. W. L., Smith, P. J. C., Winter, W. T., Arnott, S., Moorhouse, R., and Rees, D. A. *J. Mol. Biol.* 1975, **95**, 359
- 22 Alexander, L. E., Northcott, M. G. and Engmann, R. J. *Phys. Chem.* 1967, **71**, 4298
- 23 Smith, G. S. *Program and Abstracts, American Crystallographic Association, Bozemann, Mont., July 26-31, 1964*
- 24 Smith, G. S. and Alexander, L. E. *Acta Crystallogr.* 1963, **16**, 1015
- 25 Steinfink, H., Post, B. and Frankuchen, I. *Acta Crystallogr.* 1955, **8**, 426
- 26 Carlström, D. and Falkenberg, G. *Acta Chem. Scand.* 1973, **27**, 1203
- 27 'International Tables for X-ray Crystallography', Kynoch Press, Birmingham 1974, Vol 4
- 28 Geil, P. H. 'Polymer Single Crystals', Interscience, New York, 1963
- 29 Keller, A. *Rep. Prog. Phys.* 1968, **31**, 623
- 30 Magill, J. H., unpublished results
- 31 Wunderlich, B. 'Macromolecular Physics', Academic Press, New York, 1976, Vol 2, Ch 7